5-2023

Survey of the Performance of 5 nm Gold Nanoparticles Within an ssDNA-Stabilized Biosensor for the Detection of Hg2+

Madalyn Zagajowski
madd_zag@att.net

Survey of the Performance of 5 nm Gold Nanoparticles Within an ssDNA-Stabilized Biosensor for the Detection of Hg^{2+}

Madalyn J. Zagajowski

ACKNOWLEDGEMENTS

This project would not have been possible if not for the opportunity and the funds allowed by the Olivet Honors Program and the Pence-Boyce Research Committee. My undergraduate research process was an unforgettable and invaluable experience thanks to those involved in such programs. I thank my faculty advisor, Dr. Bruce Heyen, for guiding me along the long and winding road, as well as the entire ONU Chemistry Department, for never ceasing to have faith in my abilities. I further extend my thanks to all ONU faculty with whom I have had uplifting conversations, and I want to express my gratitude specifically to Dr. Nichole Vander Schaaf and Dr. Ryan Himes, who were incredible Honors mentors and always went out of their way to assure me I was doing well in navigating my project. Finally, I express my gratitude to my mother, who has always cheered me on from the sidelines in all my academic endeavors and was there for me for all those times I felt like giving up. I am truly grateful for all the support I have received thus far, and I certainly would not have come this far on my own. Thank you all for your unending encouragement.

ABSTRACT

The formation of a fluorescent biosensor complex consisting of 5 nm diameter gold nanoparticles (AuNPs) and single-stranded DNA (ssDNA) was conducted using a low-cost, efficient binding method. The analytical potential for the complex to detect mercuric ions (Hg^{2+}) in an aqueous solution was assessed through the collection of UV-vis and fluorescence spectrometry data for the AuNP-ssDNA complex. The researcher aimed to investigate this potential in case the nanoparticles formed utilizing this method were too small to result in detectable fluorescence. To eliminate this possibility, the complex synthesized from this specific method was qualitatively evaluated to determine if it consistently and reproducibly provides results that would be clearly indicative of the presence of Hg^{2+}. It was discovered that samples of the mercury-bound complex did not yield a consistent quenching for the fluorescence peak observed, as the peak height possessed a high standard deviation for the relatively small mean intensity. In addition, the methods for confirming the formation of the complex itself were not successful in showing a clear result.

Keywords: Gold nanoparticles, AuNPs, ssDNA, mercury, fluorescence spectroscopy, UV-vis spectroscopy, exonuclease I, thymine

INTRODUCTION

With the furtherance of industrialization, mercury (in addition to several other toxic heavy metals) has become a widespread environmental contaminant. Mining, smelting, consumption of fossil fuels, and other man-made processes have resulted in the release of mercury vapor into the atmosphere, where it later accumulates into water sources and sediments by wet and dry deposition (Ali et al., 2019). This contaminates the water as well as the marine life present in such water. Aquatic microorganisms absorb the settled mercury and process it into methylmercury or dimethylmercury, which are forms of mercury even more hazardous to biological systems. Fish and other marine life consume these microorganisms, which causes the mercury to be moved through food chains (Millward et al., 2019, Bernhoft, 2012). This results in the possibility of mercury poisoning from the consumption of contaminated seafood.

Mercury contaminating the environment places humans and animals at higher risk for mercury poisoning, which often causes irreversible damage to the central nervous system due to its effects as a neurotoxin. Acute exposure results in neurological damage, seizures, vomiting, diarrhea, and necrosis of the gut mucosa, whereas chronic exposure may cause fatigue, tremors, personality changes, delirium, and hallucinations in addition to neurological damage (Bernhoft, 2012). Therefore, the accumulation of these metals in our ecosystem presents a health hazard to many forms of life, as is evident by events that have occurred in the past. The major mercury disaster that took place around Minamata Bay, Japan in the 1960s is such an example. At that time, mercury deposits leaked into the bay from a chemical plant and caused many to fall victim to what was named “Minamata Disease” (2002). In addition, the state of California still struggles with the number of fish contaminated by dangerous levels of mercury in its waters as a result of the large amount of mercury released in mines during the Gold Rush. To minimize poisoning cases, the government must provide guidelines for the consumption of fish for its citizens (Alpers et al., 2005).

In the face of these continuing issues, a proper method for detecting mercury that is low-cost and efficient is being researched in order to find contamination and prevent access to contaminated water or marine life before any mercury poisoning cases result. This is highly important due to the permanence of mercury poisoning symptoms. A method that has been researched for some time is the use of a biosensor, a device that combines a biological molecule with a substance that produces a signal proportional to an analyte in some fashion. The benefits of using these biosensors include that they are selective to a targeted toxic metal (Chen et al., 2016) and they are relatively low-cost (Khoshbin et al., 2018). As a result, there has been much progress in developing them in recent years for common use (Qing et al., 2019). Several types of biosensors have been researched for the detection of heavy metals, including a family of biosensors that utilizes the fluorescent properties of metal nanoparticles. Gold nanoparticles (or AuNPs) are among the researched subjects for this purpose, and they have proven to be majorly useful in biochemical detection methods due to their binding capabilities with many biological molecules and their conductivity (Jiang et al., 2018). Therefore, they are often researched for their abilities as a fluorescence biosensor component.

Gold nanoparticle-based biosensors rely on the fluorescence that the particles emit. However, like any nanoparticle, AuNPs must be stabilized so that they do not form larger lattice structures of gold. Although this is done by the initial chemicals used to synthesize the AuNPs (such as sodium citrate), these chemicals do not provide a means for the AuNPs to fluorescently detect something such as mercuric ions (Hg^{2+}). This is the purpose of the biochemical component of the biosensor: to stabilize the AuNPs while also allowing for interaction with mercuric ions. This may be accomplished by binding a biological molecule of some type to them (Yang et al., 2020). The fluorescence of the AuNPs tends to change if the biological molecule is allowed to interact with an analyte that is a fluorescence quencher, such as mercuric ions. Therefore, this fluorescence change may be an indicator of the presence of mercuric ions (Li et al., 2018).

Because a mercuric ion will spontaneously bind with thymine (one of the four types of nucleotide bases found in DNA) and cause the formation of a T-Hg-T dimer (Park et al., 2010), an effective biological molecule to choose for AuNP stabilization would be a single-stranded DNA (ssDNA) oligonucleotide consisting only of thymine bases. A problem to overcome using ssDNA, however, is that the charges of AuNPs and DNA are both overall negative, and so they do not spontaneously bind (Liu & Liu, 2017). The most common way to allow for the interaction to take place is to use thiol-modified DNA, although this is a time-consuming process that requires removing a disulfide bond cap through column purification (Liu & Liu, 2017). Fortunately, there have been other potential methods developed that require significantly less time and resources, including a method for attaching ssDNA to AuNPs developed by Yang et al. (2006). This group found that the interaction between AuNPs and ssDNA is size-dependent; if the AuNPs are small enough (around 5 nm or less in diameter), then the DNA may be able to spontaneously attach to the surface of the AuNPs. This only requires the addition of sodium borohydride solution when the researcher synthesizes the gold nanoparticles, so this binding method would be both simple to perform and lower in cost. The concern with this method is that the fluorescence might be too small to detect easily, as the fluorescence of gold nanoparticles appears to increase with size (He et al., 2008). The question, then, is if this method allows for a sufficient signal-to-noise ratio that is both detectable and reproducible.

To address this question, this project focused on the construction of a biosensor for mercuric ion detection based on AuNPs and poly(30)T-ssDNA by use of the method performed by Yang et al. (2005). The indication that the AuNPs have been stabilized by the ssDNA is that the solution experiences a red shift in absorbance of 4-6 nm on a UV-vis spectrum (Yang et al., 2005), and so this was evaluated with a UV-vis spectrometer. Finally, the fluorescence difference between mercury-bound and non-mercury-bound ssDNA-AuNP complexes was qualitatively analyzed to determine if the sensor complex could be used to detect mercury in contaminated water and to determine if the signal produced could be analyzed quantitatively.

METHODS

Materials

Gold (III) chloride ($AuCl_3$) for preparing chloroauric acid solution, Poly(30)T ssDNA oligonucleotides, exonuclease I, sodium citrate dihydrate, sodium borohydride, and mercury (II) chloride were purchased from Sigma-Aldrich. All UV-vis data was taken using a Shimadzu UV-1280 spectrophotometer, and all fluorescence data was taken using a Hitachi F-2500 fluorescence spectrophotometer.

Synthesis of 5 nm gold nanoparticles

Gold nanoparticles of around 5 nm in diameter were synthesized and stabilized in a similar fashion to the traditional sodium citrate method (Agunloye et al., 2018). Initially, 10 mL of 1 mM aqueous $HAuCl_4$ solution was mixed with 0.8 mL of 38.8 mM aqueous solution of sodium citrate. Under vigorous stirring, 0.3 mL of an aqueous solution of 0.1 M $NaBH_4$ was added dropwise to the AuNP colloidal solution, which caused the solution to change to a vibrant red, indicating the successful formation of AuNPs of around 5 nm in diameter. The solution was then allowed to age for twenty-four hours before further use, to allow for any residual $NaBH_4$ to decompose.

Preparation of Hg-bound ssDNA samples

Mercury-bound Poly(30)T ssDNA oligonucleotides were prepared. For each sample, 15 µL of 10 µM solution of the ssDNA was mixed with 15 µL of 10 µM aqueous $HgCl_2$ solution and incubated for thirty minutes at 37 °C. Then, 8 U of exonuclease I was added to each of the solutions, and the incubation was carried out for an additional thirty minutes at the same temperature to allow for enzyme digestion of any unbound ssDNA strands (Li et al., 2019). Only one concentration of $HgCl_2$ was tested due to time constraints.

Spectral analysis

One milliliter aliquots of the AuNP hydrosol were stabilized by either Hg-bound or non-Hg-bound ssDNA and prepared for spectroscopy. The samples were prepared by combining 10 µL AuNP hydrosol, 60 µL of ssDNA (either bound to Hg or not), and 930 µL of N-2-hydroxyethylpiperazine-N'-2-ethanesulfonic acid (HEPES) buffer (0.1 M, pH 7.0). The samples were then aged for at least three hours. An absorbance spectrum for each aliquot was generated using UV-vis spectroscopy in order to locate the red shift and the highest peak of absorbance. Fluorescence data was taken by exciting at the peak absorbance wavelength to investigate any significant fluorescence intensity peaks from 530 nm-800 nm.

RESULTS

UV-vis spectroscopy

As seen in Figure 1, the average maximum absorbance wavelength for the control AuNP samples was found to be around 518 nm. A red shift was observed in only one of the non-Hg-bound ssDNA samples, contrary to what was expected. However, the red shift did appear in all the Hg-bound samples (AuNP-ssDNA complexes with Hg bound to the thymine of the ssDNA). These samples had lower absorbance, with a peak maximum around 524 nm. Samples of the UV-vis spectral data for each type of aliquot are displayed graphically below.

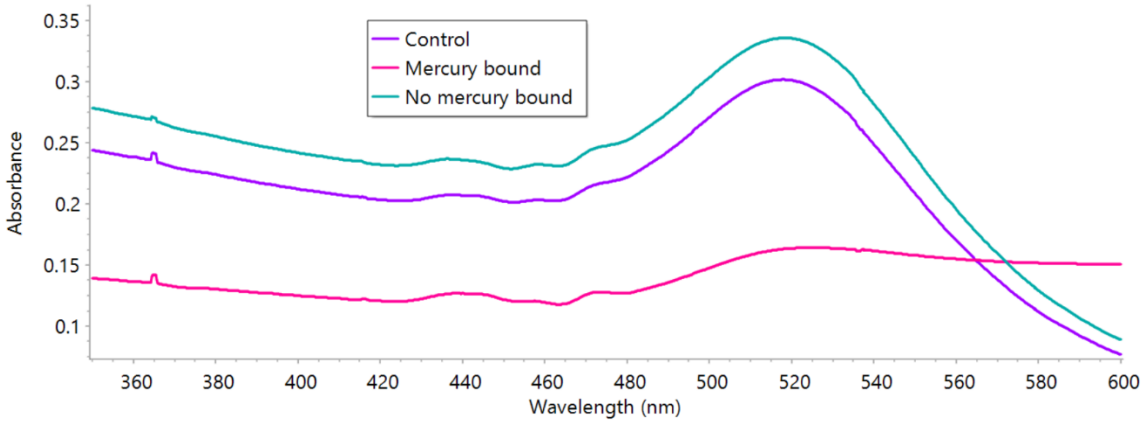

Figure 1: UV-vis spectra of the AuNP-ssDNA complex samples.
Each spectrum represents one of a sample triplicate that remained closest to the average absorbance and wavelength. The spectrum labeled "mercury bound" refers to a sample of AuNP-ssDNA complexes that have had mercury bound to the thymine along the ssDNA. The spectrum labeled "no mercury bound" refers to a sample with no mercury attached. Finally, the control line refers to a sample of AuNPs with no ssDNA complexed with them.

The average absorbance intensity at the maximum wavelength for each of the sample types are given in Table 1. Each sample was run in triplicate, and standard deviations are reported.

Table 1: Summary of finding for the UV-VIS spectra

Sample type	Control	No mercury bound	Mercury bound
Absorbance	0.302	0.344 ± 0.0087	0.160 ± 0.0059
Wavelength (nm)	517.4	518.04 ± 0.30	524.1 ± 0.81

Fluorescence spectroscopy

As seen in Figure 2, the excitation wavelength for fluorescence spectroscopy was 518 nm for the non-Hg samples and 524 for the Hg-bound samples, as these were the maximum wavelengths observed in UV-vis spectroscopy. The fluorescence spectrum of the samples showed one significant emission peak at around 791 nm. The peak was not present in a control sample of DI water, and there was a general quenching of this peak observed in the Hg-bound samples. However, the variation between samples of the same nature was rather large. Therefore, the difference between the peak height for Hg-bound samples and the peak height for non-Hg-bound

samples was not consistent. Samples of the fluorescence spectral data that were closest to the average are displayed graphically below.

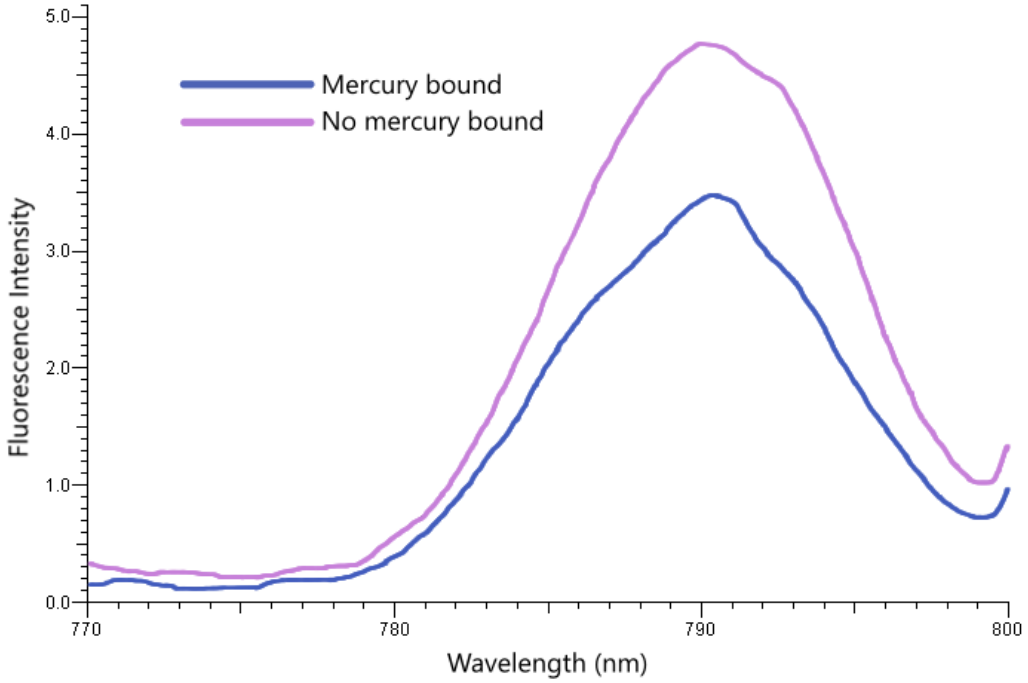

Figure 2: Fluorescence spectra of the AuNP-ssDNA complex samples.
The spectra line labeled "mercury bound" refers to a sample of AuNP-ssDNA complexes that have had mercury bound to the thymine along the ssDNA. This sample was run in triplicate and the spectrum displayed corresponds with the sample closest to the average emission intensity and wavelength. The line labeled "no mercury bound" refers to a sample of unbound AuNP-ssDNA complexes. The control is not pictured, as it was a sample of DI water that did not display any fluorescence.

The average fluorescence intensity and wavelength for each of the sample types is listed in Table 2 below. The standard deviations are reported. The mercury-bound samples were run in triplicate. However, only one sample without mercury was tested due to time constraints, so no standard deviation is included. This is an admitted shortcoming of the current project.

Table 2: Summary of findings for the fluorescence spectra

Sample type	**No mercury bound**	**Mercury bound**
Fluorescence Intensity	4.94	3.777 ± 0.71
Wavelength (nm)	790.7	790.8 ± 0.29

DISCUSSION

The evaluation of the ability of a gold nanoparticle-single-stranded DNA complex to detect mercuric ions using the binding method by Yang et al. was moderately successful. UV-vis spectra

of the complexes were obtained to find the peak absorbance and to identify the presence of a red shift. Fluorescence spectra were measured to determine if the complexes consistently produced a lower level of fluorescence intensity when mercury was bound to the thymine in the ssDNA. The data have certain implications that were not expected and are discussed below.

Fluorescence of the AuNP-ssDNA samples

The fluorescence intensity was inconsistent for the peak observed at 791 nm and only seemed to loosely follow the trend of being quenched with the addition of mercury (as seen in Table 2). The heights of the peaks seem to be even lower than that of commonly reported peak heights for 5 nm AuNPs, as well (Zuber et al. 2016), though this may be due to differences in instrumentation. The general ratio of the peak heights for both sample types was close to 1, which indicates that the difference in the peak heights is small. This fact, along with the size of the peaks themselves not being very large (only 3-5 counts of emission intensity), presents some difficulty in the determination of mercury in the sample. Therefore, if this level of variation in the peaks were to continue in the preliminary testing of this biosensor, it would be difficult to determine if a lower signal indicates there is mercury present or if it is due to the inconsistency of the peaks. Furthermore, there were no other significant peaks observed in the spectral data. With the evident non-reproducibility of the Hg-bound samples, the biosensor may fail to meet the demands required to accurately detect mercury presence and/or quantify it. It is also not known whether the peak observed is due to the fluorescence of the nanoparticles, or of something else entirely, especially since it was a rather small peak and a considerable distance from the excitation wavelength. Regardless, a sufficient biosensor must be consistent in its analytical properties, which this AuNP-ssDNA complex did not appear to display.

There are a few possible explanations for the ineffectiveness of the biosensor synthesized in this project, the most likely of which being that the gold nanoparticles are simply not large enough to produce a detectable fluorescence signal. The size of the AuNPs is crucial for Yang et al.'s method to be successful, since the method had also been attempted with larger AuNPs (of 17 nm diameter). It was found that the ssDNA did not interact with the AuNPs in that case. Therefore, the interaction is size-dependent, and smaller particles are necessary (Yang et al., 2006). As for using the complexes formed from this exact method as a biosensor component, it is very possible that the signal it produces is so small that it does not readily appear on the fluorescence spectral data. If this is the case, then the peak observed at 791 nm could be due to another component of the mixture, which could explain the reason for the inconsistency of the peak intensity relative to the presence of mercury. However, it is unknown what could be causing the peak to appear other than the AuNPs. Due to these overall fluorescence results, the binding method used for this project may inherently produce insufficient complexes for the purpose of detecting mercuric ions.

Unfortunately, there were time constraints on creating and studying samples of different concentrations in order to observe the fluorescence quenching effect. Thus, future researchers may find it helpful to perform this procedure with varying concentrations of mercury. If this is performed, a standard curve of concentration versus fluorescence quenching may be generated, and the quantification abilities of the biosensor may be observed. It is apparent from the data, however, that the mercury presence did not alter the fluorescence peak significantly or consistently under the current experimental conditions.

UV-Vis data of the AuNP aliquots

Based on the UV-vis data, there is reason to suspect that the Hg-bound DNA affected the nanoparticles, since the UV-vis spectra showed every sample processed with Hg-bound ssDNA had a significantly lower light absorbance than the samples with no mercury. The red shift also occurred in the Hg-bound samples, suggesting that the AuNP-ssDNA complex had been formed. What is peculiar, however, is that only one of the non-Hg-bound samples produced a red shift. It was even more peculiar to not observe the shift in most of the non-Hg-bound samples, as the procedure performed for these samples was the same as the method for those prepared in Yang et al.'s work, which did produce successful red shifts with their samples at similar wavelengths and intensities. The possibility of an unknown, consistent error in the non-Hg-bound sample preparation is unlikely, as procedures were strictly adhered to, but the possibility of experimental error cannot be discarded based on this data.

The diminished absorbance observed for the Hg-bound samples is an interesting phenomenon that warrants discussion. One possible reason for this observation involves absorbance shadowing. There was more than simply mercury added to the samples, as molecules of exonuclease I were still present. Being a macromolecule, exonuclease is large in comparison to some of the other components in the mixture. This may be more of a problem for this procedure as opposed to procedures that use larger gold nanoparticles, as 5 nm AuNPs are closer in size to the exonuclease. As a result, absorbance shadowing (a phenomenon in which large molecules block the light that a UV-vis spectrometer shines through a sample, keeping the light from striking smaller molecules) may be a possibility in this case, which would explain the lower absorption of the sample. This would be a problem because it is necessary for the AuNP-ssDNA complexes to absorb as much of the radiation as possible so that the fluorescence can be produced. A small fluorescence response can produce an inadequate signal-to-noise ratio for good results. Based on this hypothesis, this method may not be suitable for producing a mercury-indicating biosensor.

In future studies, it may be worth researching the lower absorbance that resulted from the mercury-bound DNA. Unfortunately, there was not enough time to create and evaluate samples without exonuclease I incubation, and this should be investigated. But in that event, the signal may have been even more difficult to interpret since exonuclease I's purpose was to eliminate background noise from the fluorescence spectral data. Regardless, if mercury was the cause of the absorbance change, then it would be important to determine if it did so by the nature of the interaction, or if it lowered the absorbance in its unbound state. Tests for the selectivity of the mercury regarding this absorbance change should be conducted as well.

Additional concerns

Finally, it was difficult to determine the correct amounts and concentrations to include in the samples for spectroscopy. The amounts and concentrations of the components of the mixture, especially the buffer, varied between the research projects that were performed with similar methods to this one (Li et al., 2018, Liu et al., 2017, Yang et al., 2006). Therefore, it is unknown whether the optimal concentrations and amounts were used in this research, which could be a source of the uncertainty of the results of the UV-vis spectrometry as well as the fluorescence spectroscopy.

CONCLUSION

In this project, the method suggested by Yang et al. did not produce a biosensor that adequately indicated the presence of mercuric ions; it is possible that the gold nanoparticles were too small to produce a detectable fluorescence signal. In addition, the red shift of absorbance that would indicate the formation of the AuNP-ssDNA complex appeared for the samples containing DNA bound to mercury, but it did not appear for the samples without mercury. This calls the validity and effectiveness of the biosensor into question. However, other methods for confirming the formation of the complex were unable to be performed due to the timeframe for this project, and these methods may be a good starting place for future research. One process to confirm the complex formation would be to conduct a polyacrylamide gel electrophoresis, in which a high molecular weight band would indicate the complex formation, while a lower molecular weight band and other visible bands would indicate no complex formation. This could not be performed within the timeframe of this project. An alternative way to confirm the formation of the complex is with TEM imaging. This type of testing might be available in the future through collaboration with other institutions. Evaluating samples with these methods would allow for a more complete picture on the complexation status of the components.

REFERENCES

Environmental Health Department, Ministry of the Environment. *Minamata Disease: The History and Measures*. Tokyo, Japan: Ministry of the Environment, Government of Japan; 2002.

Agunloye, E., Panariello, L., Gavriilidis, A., & Mazzei, L. (2018). A model for the formation of gold nanoparticles in the citrate synthesis method. *Chemical Engineering Science*. 191, 318–31.

Ali, H., Khan, E., & Ilahi, I. (2019). Environmental chemistry and ecotoxicology of hazardous heavy metals: environmental persistence, toxicity, and bioaccumulation. *Journal of Chemistry*. 6730305.

Alpers, C. N., Hunerlach, M. P., May, J. T., & Hothem, R. L. (2005). Mercury Contamination from Historical Gold Mining in California. *U.S. Geological Survey.* 2005–3014.

Bernhoft R. A. (2012). Mercury toxicity and treatment: a review of the literature. *Journal of Environmental and Public Health*. 460–508.

Chen, J., Ji, X., Tinnefeld, P., & He, Z. (2015). Multifunctional dumbbell-shaped DNA-templated selective formation of fluorescent silver nanoclusters or copper nanoparticles for sensitive detection of biomolecules. *ACS Applied Materials & Interfaces.* 8, 1786–94.

He, H., Xie, C., & Ren, J. (2008). Nonbleaching fluorescence of gold nanoparticles and its applications in cancer cell imaging. *Analytical Chemistry*, *80*(15), 5951–57.

Jiang, P., Wang, Y., Zhao, L., Ji, C., Chen, D., & Nie, L. (2018). Applications of gold nanoparticles in non-optical biosensors. *Nanomaterials (Basel).* 8(12), 977.

Khoshbin, Z., Housaindokht, M.R., Verdian, A., & Bozorgmehr, M.R. (2018). Simultaneous detection and determination of mercury (II) and lead (II) ions through the achievement of novel functional nucleic acid-based biosensors. *Biosensors and Bioelectronics*. 116, 130–47.

Li, J., Fu, W., Bao, J., Wang, Z, & Dai, Z. (2018). Fluorescence regulation of copper nanoclusters via DNA template manipulation toward design of a high signal-to-noise ratio biosensor. *ACS Applied Materials & Interfaces*. 10(8), 6965–71.

Liu, B. & Liu, J. (2017). Methods for preparing DNA-functionalized gold nanoparticles, a key reagent of bioanalytical chemistry. *Analytical Methods*. 9, 26–33.

Millward, G.E., Turner, A., & He, X. (2019). Metal pollution. *Encyclopedia of Ocean Sciences (3rd ed.).* Elsevier Science & Technology.

Park, K.S., Jung, C., & Park, H.G. (2010). “Illusionary” polymerase activity triggered by metal ions: Use for molecular logic-gate operations. *Angewandte Chemie International Edition*. 49(50), 9757–60.

Qing, Z., Bai, A., Xing, S., Zou, Z., He, X., Wang, K., & Yang, R. (2019). Progress in biosensor based on DNA-templated copper nanoparticles. *Biosensors and Bioelectronics.* 137, 96–109.

Yang, J., Lee, J.Y., Too, H.P., Chow, G.M., & Gan, L.M. (2006). Single stranded DNA stabilization and assembly of Au nanoparticles of different sizes. *Chemical Physics*. 323(2), 304–12.

Yang, M., Chen, X., Su, Y., Liu, H., Zhang, H., Li, X., & Xu, W. (2020). The fluorescent palette of DNA-templated silver nanoclusters for biological applications. *Frontiers in Chemistry*. 8, 601–21.

Zuber, A., Purdey, M., Schartner, E., Forbes, C., van der Hoek, B., Giles, D., Abell, A., Monro, T., & Ebendorff-Heidepriem, H. (2016). Detection of gold nanoparticles with different sizes using absorption and fluorescence-based method. *Sensors and Actuators B: Chemical*. 227, 117–27.